Investigation of PWM Controlled, Resonant Transition Converters with Asymmetrical Duty Cycle

Norbert Fröhleke, Alfred Fiedler, Horst Grotstollen

Institute for Power Electronics and Electrical Drives
University of Paderborn, FB14
Postfach 1621
33098 Paderborn, Germany
Tel.: ++49 – 5251 – 60 3157, FAX: ++49 – 5251 –603157
E–mail: froehleke@pblea.uni-paderborn.de

Bassile Margaritis

ABB CEAG Stromversorgungstechnik

Postfach 78
59494 Soest, Germany
Tel.: ++49 – 2921 – 69582, FAX: ++49 – 2921 – 69399

Abstract — **Investigations on a specific group, the asymmetrical duty cycle controlled power converters, which belong to the class of resonant transition topologies are presented. A detailed analysis following a state–graph strategy is given, revealing three modes of operation. Various design equations are derived representing the equipment for a consolidated design of a 300V–5V/60A dc/dc-converter, switched at 500KHz. The high measured efficiency of 86% at rated power and up to 89% at half load, resulting due to high turns ratio and low reactive power, proves this switching technique favorable as compared with other soft switching techniques of the last decade by eliminating switching losses without rise of conduction losses.**

I. INTRODUCTION

Broad comparisons between PWM–, Quasi–resonant and resonant converters were conducted reported to literature in [1] and [2] based on an approximated circuit behavior in order to yield optimum topologies for specific applications. The search for more efficient operating circuits aims in this case on high power density dc/dc converters built in dense packaging technology for power modules. However, raising the efficiency and power density goes along with a reduction of reactive power and minimization of components in the power rail.

That is the reason why in industry hard switched PWM controlled converters still dominate the SMPS field despite the flood of publications from university researchers and thus, several authors [3, 4, 5] still favor standard PWM converters using regenerative snubbers for switching stress reduction, which are not charged by the heavy real power flow. But still the application of snubbers leads mostly to non–negligible charge–down losses in case of supplying dc/dc–converters out of mains voltage for high power modules instead of being supplied by a low grid voltage of 48V in today distributed supply architectures.

A switching technique, known by today, wherefrom a boosting of efficiency can still be expected is the resonant transition class of converters as e.g. reported in [6]. Generally, a resonant switching or the so called „resonant transition converters“ utilize inherent commutation means like leakage inductance of a transformer and transistor capacitances or extra discrete components for commutation which are to be added to the circuit in order to soften the switching transitions. Logically, especially these added commutational means can be combined with auxiliary switches as was taught since 1935 in textbooks by Glaser, then Wasserab, Meyer etc. With the availability of power semiconductors with the capability to switch–off at always higher apparent switching power levels the necessity to use commutational means has moved from the strict constraint towards using it only for the reduction of switching stress and losses that higher switching frequency may lead towards higher power density or to reduce the weight or simply EMI. Resonant transition switching combines the best features of resonant with conventional hard switched PWM converters by reducing switching losses, while maintaining low conduction losses and constant switching frequency with its positive effects on EMI–filtering.

The use of an „active clamp“ given by Vinciarelli which minimizes EMI, switching losses due to the occurrence of zero voltage switching (ZVS) in a certain operation area and allows a duty cycle in excess of 50%, whereby the transformer turns ratio can be increased for lower conduction losses of the active switch and the diodes as less blocking voltage results, was selected during the last years by a number of authors like Watson, Hua, Jitaru etc. for small medium power applications (e.g. 100...600 W). In total, the circuit features a number of positive attributes as already mentioned and can be considered to belong to the resonant transition class of converters. Another positive criterium is that the MOSFET voltage is relatively constant for different load and line conditions but high in magnitude and that the transformer is simple with only two windings allowing positive and negative magnetic flux excursions in the first and third quadrant of the B–H characteristic; thus, at first sight a higher core utilization results.

This „current mirror demagnetization“ as originally called by Vinciarelli obtains an inherent negative feedback against core saturation, reflecting the magnetizing current after some switching intervals (depending on the magnetizing inductance, clamp capacitor and operation point)

This work was sponsored by a research contract with ABB CR–Heidelberg and ABB CEAG Stromversorgungstechnik–Soest.

towards the voltage of the clamp capacitor. For example, if the output voltage drops as consequence of a positive step current load the voltage–time product on the primary winding increases following an enlarged duty cycle by the controller, thus, increasing the magnetizing current. But as the clamp voltage cannot reflect this excursion of the current during the next switching cycle, due to the low resonant frequency determined by the magnetizing inductance and the clamp capacitor, the magnetizing current rises and after a transient period the clamp voltage reflects again the new magnetizing condition at steady state. That is the reason, why the useful swing of the flux density is low and gives a fine tuning task on the design of the transformer, clamp capacitor and an additional saturable inductor in series with the forward diode. This saturable inductor temporarily disconnects the transformer from the load after the auxiliary switch is turned off in order to utilize the entire magnetizing current for discharging the output capacitance of the main transistor. In addition to this negative aspects summarized above one has to add that its output filter is still larger as compared to bridge topologies due to its single ended nature and that it is less suitable for applying synchronous rectifiers, as the transitions of the controlling secondary voltage of the transformer are less sharp.

The group of asymmetrical duty cycle controlled bridge converters (as reported in [7]), representing one subgroup within the resonant transition class is capable of lowering input current pulsation, whereby the still bulky input filter can be minimized. By means of a high turns ratio of the transformer resulting from rapid transitions the inverter losses are reduced considerably, leading to higher efficiency as compared to optimized Quasi–Resonant Converters and their PWM counterparts, reported in [10].

II. PRINCIPLE OF OPERATION

Assuming an isolated bridge type standard PWM converter as shown in Fig. 1 is operated at 50% duty cycle D with only enough dead–time for voltage commutation of the switches, then this circuit will show soft switching as long as the stored energy in the leakage inductance of the transformer or any commutation inductor is sufficient to swing the switch voltages (indirectly given by the bridge diagonal voltage u_p of Fig. 2) together with precise switch turn–on timing. At low current levels the stored magnetic energy is too low to guarantee lossless transitions, just as in resonant pole converters. If the stored energy is too high, then the extra energy is delivered back to the source, just like in resonant converters with lagging tank current (operation above resonance frequency). The boundary between soft and hard switching depends of course on the ratings of parasitic transistor capacitances, the commutating inductance and the load resistance, indicated by a sharp decline in efficiency, when the lossy switching mode is entered. This switching scheme is exploited e.g. in [8] with the disadvantage of lost controllability at constant D of 0.5. But this is regained, when switching is performed with an asymmetrical duty cycle.

Fig. 1 shows a halfbridge topology with transistors Q_d and Q_c gated by waveforms depicted in Fig. 2. The capacitance values of C_a, C_b are large to yield near constant voltages. The voltage across the diagonal of the bridge u_p is transformed, rectified and filtered by an LC–output filter. The fullbridge topology requests a series capacitor too, to stabilize the magnetizing current of the transformer. But as low loss, low volume MLC capacitors are cheaply available today, even for larger rms–current loadings this component does not represent a series drawback any longer when compared to single ended converters or the paralleling of e.g. two forward converters to yield the same filter size. The resulting transformer core utilization in single ended topologies is of course far lower than with bridge topologies. The control law with duty cycle $D = T_d/T$ and $D_c = T_c/T$ is derived for a lossless circuit at steady state, i.e. balanced volt–seconds on the transformer's primary winding:

$$U_a \approx \frac{2pU_i}{n} D\,(1-D) \tag{1}$$

$$D \approx \frac{1}{2}\left(1 \pm \sqrt{1 - \frac{2n \cdot U_a}{pU_i}}\right) \quad \text{with} \quad p = \begin{cases} 1 \ ; \ \text{ASHB} \\ 2 \ ; \ \text{ASFB} \end{cases} \tag{2}$$

Approximations (1) and (2) converge to equations, if the magnetizing current i_m of the transformer is negligible and the slope of the primary current i_b is constant. The latter

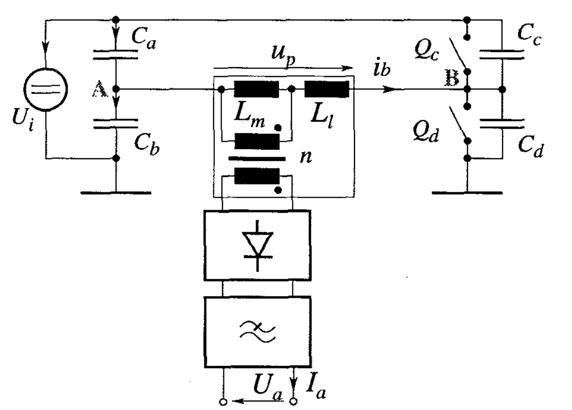

Fig. 1: Typical halfbridge topology whereby the shaded box represents the transformer with leakage and magnetizing inductance.

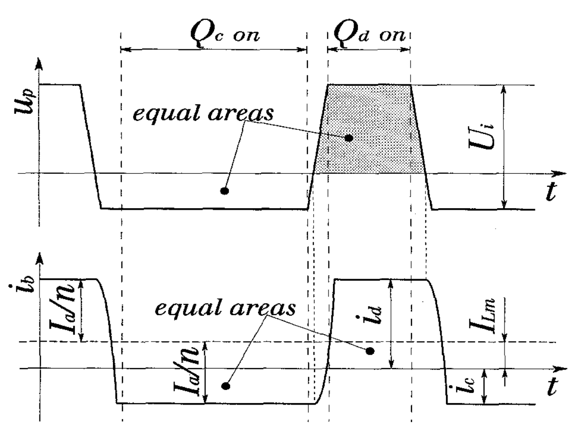

Fig. 2: Typical waveforms for the ASHB at soft switching (mode I)

assumption is very near to the real behavior. Equs. (1) and (2) describe a parabolic relation between D and voltage ratio $M = U_a/U_i$ but reasons of definity limit D to $0 < D < 0.5$ here.

The ac–component of the magnetizing current calculates to:

$$\Delta i_m \approx \frac{U_a \cdot n}{2p \cdot L_m \cdot f_s} \quad \text{with } f_s = \text{switching frequency}. \tag{3}$$

Application of Kirchhoffs laws and conditions for steady state yield a dc–component of the magnetizing current:

$$\bar{i}_m \approx \frac{1}{n} I_a (1 - 2D) \ . \tag{4}$$

The analysis of the soft switching converter including parasitic transistor capacitances (C_c, C_d in a halfbridge, see Fig. 1) and commutation inductance L_l is treated in the next chapter.

III. ANALYSIS OF THE ASYMMETRICAL DUTY CYCLE CONTROLLED HALFBRIDGE

For the analysis of the ASHB including those components, the soft switching is based on we assume that the circuit elements are free of losses and that the output filter current is ideally filtered, assuming C_a=C_b, C_c=C_d defining

$$\frac{1}{2C_c} + \frac{1}{2C_a} = \frac{1}{C_g} \quad \text{and} \quad L_m + L_S = L_g \tag{5}$$

and use of Kirchhoffs Laws yield with L and C as state depending equivalent quantities

$$i_b(t) = i_{b0} \cos\left(\frac{t}{\sqrt{LC}}\right) + (u_{C30} - u_{C10}) \sqrt{\frac{C}{L}} \sin\left(\frac{t}{\sqrt{LC}}\right) \tag{6}$$

with i_{b0}, u_{Ca0} and u_{Cd0} as initial values for the respective intervals. Integration of (6) and consideration of u_{Ca0} and u_{Cd0} gives the switch voltages $u_{Ca}(t)$ and $u_{Cd}(t)$:

$$u_{Ca}(t) = \frac{-1}{2C_3}\left[i_{b0} \sqrt{LC} \sin\left(\frac{t_i}{\sqrt{LC}}\right) - (u_{Ca0} - u_{Cd0})\, C \left(\cos\left(\frac{t_i}{\sqrt{LC}}\right) - 1\right)\right] + u_{Ca0} \tag{7}$$

$$u_{Cd}(t) = \frac{-1}{2C_3}\left[i_{b0} \sqrt{LC} \sin\left(\frac{t_i}{\sqrt{LC}}\right) - (u_{Ca0} - u_{Cd0})\, C \left(\cos\left(\frac{t_i}{\sqrt{LC}}\right) - 1\right)\right] + u_{Cd0} \tag{8}$$

with t_i as time duration. Equations above are evaluated using initial values, calculated by a state–graph strategy [9] as illustrated in Fig. 3. Three modes of operation were derived characterized as follows:

A. High power soft switching mode (mode I)

Zero–voltage switching occurs, as for high power the energy stored in the commutating inductor is sufficient to swing the switch voltage (see Fig. 6). At instant t_o switch Q_d opens *(state Z6)*. Thus C_d is charged, C_c is discharged *(state Z2a)* by i_b until $u_p(t_1) = 0$, whereby the free wheeling *state Z3a* is initiated.

All secondary sided diodes share the constant filter current I_a, shorting the transformer with magnetizing current i_m (current through L_m) remaining constant. C_c is discharged at t_2 forcing the antiparallel diode of Q_c to conduct, whereby a relatively small amount of energy stored in the commutation inductance L_l as compared with resonant converters is returned to the source.

This can be viewed as one of the reasons for the increased efficiency, documented in Fig. 8. Hence Q_c switches on at zero voltage *(Z3a –> Z11)*, terminating the commutation from Q_d to Q_c. But interval II in Fig. 5 is not yet terminated, until i_b equals the magnetizing current plus reflected load current. After the commutation of the load current from one secondary sided diode to the other the transformed output current is reflected to the primary with opposite polarity at state III *(Z9)*, which is the major power transfer interval during the first half–cycle. As the potential at node A is fixed u_p equals u_{ca}.

Interval III is terminated by the actual duty cycle D, when Q_c switches off and Q_d on – after a short delay time. The second half cycle is developed analog to the first, reminding that the duration differs of course.

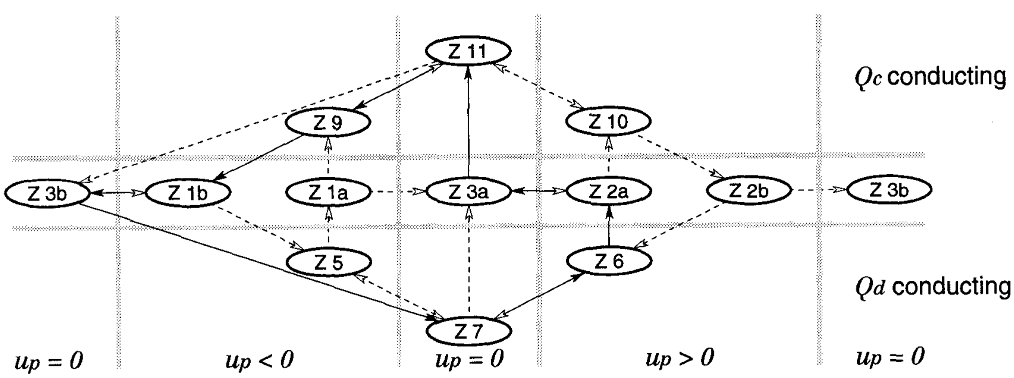

Fig. 3: Solution strategy by state-graphs, indicating states and modes of operation at
a) high power, soft switching (mode I ——) b) low power, hard switching (mode II e.a. - - -)

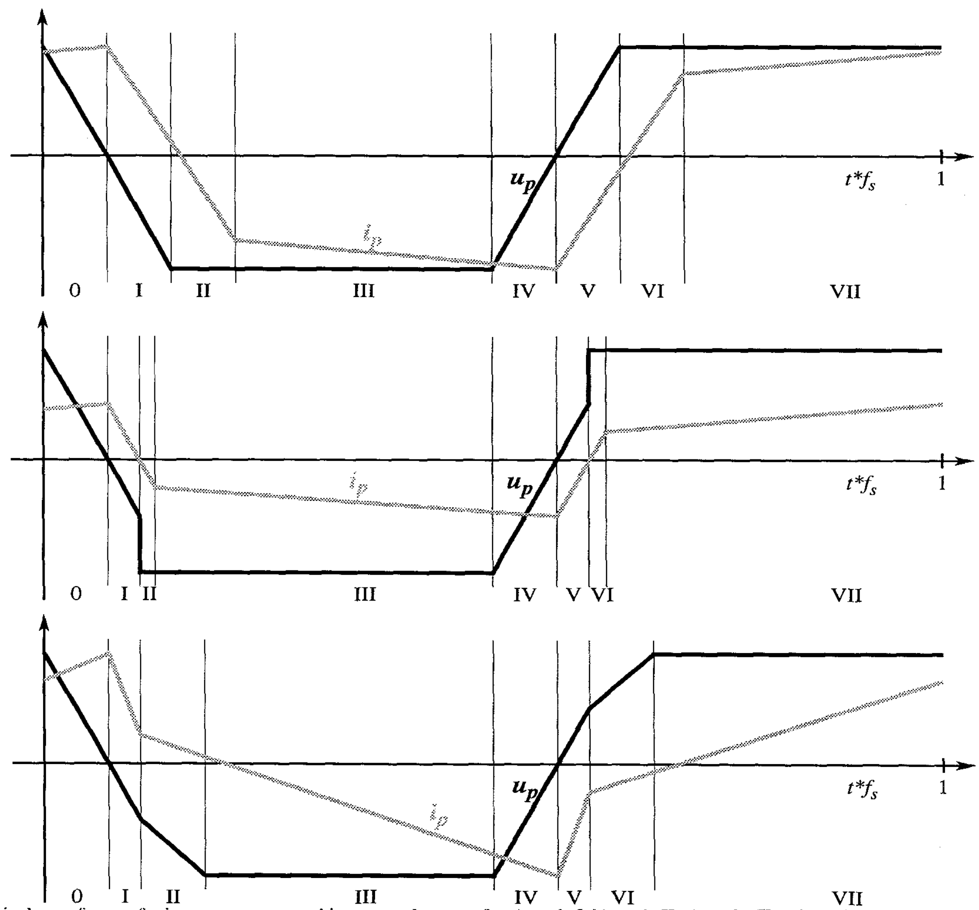

Fig. 4: Principal waveforms of primary current i_b and inverter voltage u_p for a) mode I, b) mode II, c) mode III and relation between intervals and states: 0=Z2a, I=Z3a, II=Z11, III=Z9, IV=Z1b, V=Z3b, VI=Z7, VII=Z6

B. Low power hard switching mode (mode II)

Starting point is once again the opening of switch Q_d *(state Z6),* which initiates the charging of C_d respectively discharging of C_c *(state Z2a).* At lower power levels the slope of u_p decreases so that i_b drops to zero at the end of state I, before charging of C_d resp. discharging of C_c has been completed. But as Q_c is gated positive *(Z10)* at this instant charge–down losses, but no recovery losses occur (see Fig. 3 and Fig. 4b) accompanied by a reduction of efficiency (see Fig. 8), when entering this lossy mode. The sequence of the other intervals is similar to that of mode I.

C. Very low power soft switching mode (mode III)

At very low power levels the transformer voltage u_p retains zero at the end of state 0, initiating the free wheeling state at Interval I. But as magnetizing current is relatively large as compared with the transformed load current, the state, characterized by a discontinuous transformer voltage is replaced again as the demagnetizing transformer affects the conduction of the opposite diode as before in the main energy transfer interval.

IV. VERIFICATION

A dc/dc converter with a wide input voltage range of 225...425V was designed for nominal output quantities of 5V/60A, switching at 0.5MHz. The leakage inductance of a planar transformer represent the total of the commutating inductor with typical sandwiched windings. The transformer design was conducted by a CAD–package developed for ABB–CEAG. The transformer characterization is given by the measured short circuit resistance depicted in Fig. 5. The volume is rated at $25x25x10mm^3$. It is intended to optimize the interleaving and the copper height even further with the

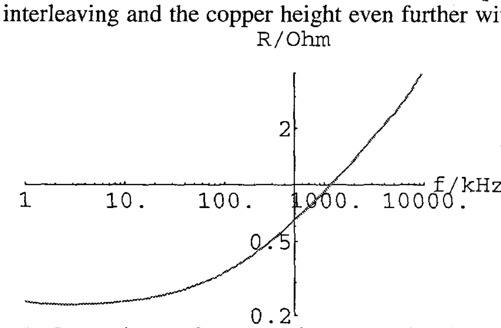

Fig. 5: Input resistance of power transformer, secondary side shorted

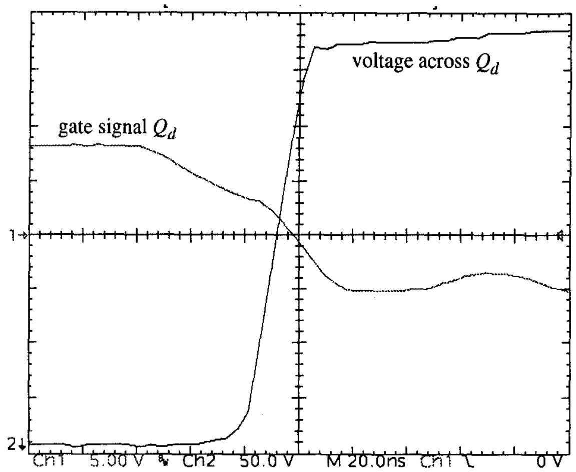

Fig. 6: Measured waveforms of ASHB at nominal power (mode I) operation conditions: 380V/5V – 60A, 500kHz

computer aided optimization tool introduced in [11]. A characteristic voltage waveform measured across Q_d and the respective gating signal is given in Fig. 6 for the soft switching mode of operation (mode I) at 60 A rated output current, whereas the variation of the positive slope of the voltage across Q_d in Fig. 7 clearly indicates that initially at the switch–off of Q_d the voltage rises slowly but then the switch–on of Q_c does not show ZVS any longer at an output current of 6A (mode II). Additionally the respective gate signal and logic signal are displayed in Fig. 7.

Note, that the high efficiency, depicted in Fig. 8 was obtained, despite the overrating of secondary sided diodes with resp. to current is low and a typical 45V double diode (IR–80CNQ045) is applied. The power consumption of the control circuitry is included in the efficiency plots given in Fig. 8. Towards low output current the drop in efficiency is due to charge–down losses when entering the hard switching mode of operation. They are of course more pronounced with higher input voltage due to higher losses and due to a larger asymmetry.

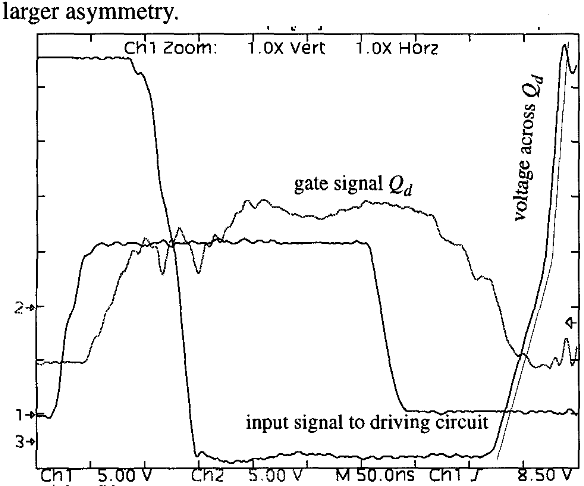

Fig. 7: Measured waveforms of ASHB at low power (mode II) operation conditions: 350V/5V – 6A, 500kHz

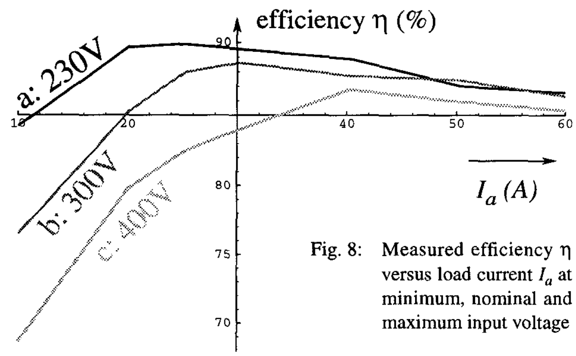

Fig. 8: Measured efficiency η versus load current I_a at minimum, nominal and maximum input voltage

V. CONCLUSION

Asymmetrical duty cycle controlled bridge topologies belonging to the group of resonant transition converters show varies modes of operation in a typical operation range when accounting for the transitions. These modes of operation are verified on a 5V/60 A dc/dc converter, switching at 0.5 MHz. The converter yields a noticeable rise in efficiency as compared to common PWM and resonant converters and power density, since the footprint of the power transformer is small and the driving scheme is simple. The unequal blocking voltage of the rectifiers is a disadvantage of the circuit.

REFERENCES

[1] R. Farrington, M.M. Jovanovic, F.C. Lee: „*Analysis of reactive power in resonant converters*", IEEE PESC 1992, pp. 197–206

[2] N. Fröhleke: „*Topologies and switching concepts for SMPS with high power and low output voltage*", Ph. D. Thesis (in German), University of Paderborn, 1991

[3] K. Nishimara et al.: „*High frequency high power converter*", PESC 1988 pp 180–187

[4] L. Heinemann, N. Fröhleke, H. Grotstollen: „*High power, high frequency quasi–zero–voltage–switched PWM forward converter with very low reactive power*", High Frequency Power Conversion Conf. (HFPC) 1993, pp. 94–100

[5] N. Fröhleke, H. Grotstollen, B. Margaritis: „*Comparison of quasi–zero voltage switched forward–converters with LCC–resonant converters*", HFPC 1994, pp. 135–151

[6] O.D. Patterson, D.M. Divan: „*Pseudo–Resonant full bridge dc/dc converter*", IEEE, Trans. on power electronics, vol. 6, no. 4, Oct. 91, pp. 671–678

[7] P. Imbertson, N. Mohan: „*New PWM converter circuits combining zero-switching loss with low conduction loss*", Proc. of the internat. Telecom. Energy Conf., 1990, pp. 179–185

[8] M. Elmore, St. Newton: „*A high power factor ac-to-dc converter for distributed power systems*", HFPC 1993, pp. 232–241

[9] A. Fiedler, H. Grotstollen: „*Stategraph method to ascertain trajectories of complex systems*" (in German), 37. Int. Scientific Colloq., 1992, vol. 1, pp. 314–317

[10] A. Lotfi, D. Sable, F.C. Lee: „*Nonlinear design optimization of Quasi Resonant Converters*", PESC 1990, pp. 66–73

[11] N. Fröhleke, B. Becker, P. Wallmeier, N. Grotstollen: „*Computer aided Optimization of Multiwinding Transformers for Switch Mode Power Supplies considering HF–effects*", IEEE Proc. IAS 1994 Vol.2, pp.1043–1048

[12] A. Fiedler: „*Contributions for the development of dc/dc converters for high power with low output voltage*", Ph. D. Thesis (in German), University of Paderborn, 1995